

Research Design and Methods

Clinical Assessments and Definitions

Fasting blood glucose, measured by the central laboratory of Heidelberg University Hospital, was recorded for all individuals in the study to assess short-term glycaemic control, while glycated haemoglobin (HbA1c) data were not available for all participants. The presence of complications, including cardiovascular disease (CVD), retinopathy, nephropathy, neuropathy, and ischemia/infection, was evaluated for each individual. CVD was defined by the presence of one or more of the following conditions: a history of myocardial infarction (>6 months prior), diagnosed coronary heart disease, percutaneous transluminal coronary angioplasty (PTCA) with stent placement, or current treatment for hypertension. These conditions were identified through a review of patient medical records. Retinopathy was diagnosed using fundoscopy. Nephropathy was assessed by calculating the estimated glomerular filtration rate (eGFR) using the Chronic Kidney Disease Epidemiology Collaboration (CKD-EPI) formula, with a cutoff of <60 mL/min/1.73 m² used to define nephropathy (1). Neuropathy was assessed using the Neuropathy Disability Score (NDS) and Neuropathy Symptom Score (NSS), following the guidelines of the German Diabetes Association (2). Ischemia and infection were classified as either localized (restricted to the affected limb) or systemic (involving generalized symptoms). The severity of ischemia was determined through clinical evaluation, with patient records reviewed for details of any prior interventions, such as revascularization or antibiotic therapy.

Electron microscopy

Isolated fascicles were cut into longitudinal segments (1 x 2 mm) and processed as previously described (3). Briefly, the dissected tissue was fixed for at least two hours at room temperature in a solution of 3% glutaraldehyde and 3% sucrose in Sörensen buffer. The tissue was then washed in Sörensen buffer and post-fixed for two hours at 4°C in 1% osmium tetroxide. The fixated tissue was then rinsed in water, dehydrated through graded ethanol solutions, transferred into propylene oxide, and embedded in epoxy resin (glycidether 100/araldit). Semithin and ultrathin sections were cut with an ultramicrotome (Reichert Ultracut E, Wien, Austria). Ultrathin sections were treated with uranyl acetate and lead citrate, and examined with a transmission electron microscope Jem1400 (JEOL) equipped with a F216 TVIPS digital camera. Ultrastructural features were visually assessed by an expert neuropathologist (J. W.).

MRI data acquisition

Images were acquired in axial orientation to the long axis of the nerve specimens. The MR protocol included the following sequences:

At 3 T MRI clinical resolution to match *in vivo* imaging findings:

1. High-resolution T2-w turbo-spin-echo (TSE) sequence at 3 T to match: 2D sequence, TE: 55 ms, TR: 7570 ms, echo train length: 13, spectral fat saturation, Field-of-View (FoV): 120 x 120 mm², acquisition matrix: 512 x 333, number of slices: 41, slice thickness: 3 mm, number of averages: 3, acquisition time: 04 min 48 s.

At 9.4 T ultrahighfield-MRI to precisely guide and localize lesioned fascicles:

1. High-resolution Rapid Acquisition with Refocused Echoes (RARE) T2-w sequence: 2D sequence, echo time (TE): 40 ms, repetition time (TR): 2500 ms, 47 µm in plane resolution, acquisition matrix: 512 x 212, slice thickness: 1 mm, rare factor 4, number of averages: 2, duration: 4 min 35 s.
2. DTI-spin echo sequence: 2D sequence, number of diffusion gradient directions: 18 + 5 A0 images, TE: 18.1 ms, TR: 1200 ms, 100 µm x 128 µm in plane resolution, acquisition matrix: 120 x 50, b-values: 0/650 s/mm², gradient duration: 2.5 ms, gradient separation:

15.5 ms, flip angle: 130°, spectral fat saturation, slice thickness: 1.5 mm, number of averages: 1, duration: 23 min 05 s.

3. Multi-Slice-Multi-Echo (MSME) sequence: 2D sequence, TE: 9.7 ms, number of echoes: 20, TR: 3200 ms, 80 μ m in plane resolution, acquisition matrix: 300 x 127, slice thickness: 1 mm, number of averages: 1, duration: 7 min 12 s.
4. T1-w Fast Low-Angle Shot (FLASH) sequence: 2D sequence, TE: 4.7 ms, TR: 350 ms, 47 μ m in plane resolution, acquisition matrix: 277 x 161, slice thickness: 1 mm, flip angle: 40°, Magnetization Transfer (MT)-pulse: 15 μ T, number of averages: 2, duration: 1 min 51 s (2x; MT-pulse on/off).

MRN Image Post-processing and Analysis

Apparent diffusion coefficient (ADC), fractional anisotropy (FA), radial diffusivity (RD), axial diffusivity (AD), magnetization transfer contrast (MTC), and T2-Time maps were calculated using a custom-written Matlab routine (R2015a, MathWorks Inc., Natwick, USA) as reported previously (3). MRN images were exported, and evaluation was performed in ImageJ/Fiji (4), as described previously (3,5). Subsequently, all individual nerve fascicles were segmented manually and segmented fascicles were further subjected to quantitative analysis of T2-time. For an unbiased classification of fascicular nerve lesions within the entire sample, a two-component Gaussian-Mixture-Model (GMM) was fitted to the overall distribution using Matlab. Based on this analysis, nerve fascicles were classified as either “non-lesioned fascicles (NLF)” or “lesioned fascicle (LF)”.

Nerve Dissection & Histological examination

Following MRN, the sciatic nerve samples were again placed on ice. The positional information of the lesion(s) obtained from the MRN was then used to guide the precise sectioning of the tissue. The region containing the lesion was then fixated and embedded in paraffin (FFPE). From each sample, sequential five-micron sections were made in which every fifth section was stained with hematoxylin and eosin (HE) and Alcian blue/periodic acid–Schiff (AB-PAS). Images were acquired using an Aperio AT2 System (Leica) and were exported and evaluated using ImageJ/ Fiji (4). The light microscopy and MRN images were aligned to establish whether the correct section(s) has been cut with respect to the presence or absence of the lesion(s). Perineural thickness and the fascicular area were measured using the standard annotation and segmentation tools, whilst a semi-quantitative AB-grade from 1 to 4 (“1”: absence of AB-positive streaks or areas; “2”: minor AB-positive streaks or areas; “3”: substantial AB-positive streaks or areas; “4”: (Sub-)total filling with AB-positive areas) was assigned to each fascicle depending on the degree of AB-positivity.

Immunofluorescence Staining

FFPE sections (5 μ m) containing the LF were stained for the following nerve fiber markers, as previously described (6): neurofilament light (NFL, Cell Signaling, 2835; 1:100), PGP9.5 (Merck, AB1761-I; 1:500) and myelin basic protein (MBP, Abcam, ab62631; 1:200). Each marker was visualized with either anti-mouse or anti-rabbit Alexafluor488 (1:1000; Cell Signaling) and counterstained with DAPI. Fluorescent images were acquired on a Nikon A1R confocal microscope and were exported and evaluated using ImageJ/ Fiji (4). For determination of the number and size of the axons, frequency distribution analysis was performed, fitting that data to a non-Gaussian curve to determine the number of the axons (=amplitude) and the size (=geometric mean).

Sample processing

Following laser dissection, collected samples underwent antigen retrieval followed by reduction/alkylation/reduction. Two steps of digestion in highly concentrated trypsin solutions

(Thermo/Pierce) were performed in the presence of 0.01% Rapigest (Waters, Milford, MA, USA). The first step of digestion was performed in a solution of trypsin at 60 µg/ml, prepared in 50mM ammonium hydrogen carbonate. The second step was performed in a solution of 30 µg/ml trypsin in 80% acetonitrile (ACN). After digestion, the samples were dried by vacuum centrifugation and desalted using C18 Solid Phase Extraction tips (ZipTip, Merck Millipore, Burlington, MA, USA). The peptides were eluted using 50% of ACN in acidified water (0.1% trifluoroacetic acid in final concentration) and dried, ready for analysis by liquid chromatography–tandem mass spectrometry.

Data Processing & Pathway Analysis

Processing of the raw data was carried out by MaxQuant (version 1.6.14.0)(7), using a human reference proteome database (February 27, 2020; 74 811 entries) extracted from Uniprot.org under default settings. Identification FDR cutoffs were 0.01 on peptide level and 0.01 on protein level. Match between runs option was disabled. Quantification was done using a label free quantification (LFQ) approach based on the MaxLFQ algorithm (8). A minimum of 2 unique peptides per protein was required for protein quantification. The LFQ intensities for the identified proteins were log 2 transformed and visualized as a heat map, and clustering was performed by R software packages, tidyverse and pheatmap. The fold changes (FC) of the proteins were calculated by comparing the NLF-T2D or LF-T2D to NLF-Ctrl. The comparison of more than one group was achieved using two-way ANOVA analysis, correcting for multiple comparisons by controlling the false discover rate (FDR; <0.05). Volcano plots were used to visualize these differences in which the cutoffs used to significantly changed proteins was $-\log_{10}(\text{adjusted p-value}) > 1.30$ and $-2 \leq \text{FC} \leq 2$. Interaction analyses were performed using STRING (<https://string-db.org/>). The finalized proteomic data set(s) were submitted into Ingenuity Pathway Analysis (IPA) for core analysis (Ingenuity Systems, Redwood City, CA). For canonical pathway analysis, disease and function, the $-\log(\text{P-value}) > 2$ was taken as threshold, the Z-score > 2 was defined as the threshold of significant activation, whilst Z-score < -2 was defined as the threshold of significant inhibition.

Statistical analysis

For statistical analysis Prism Version 7.02 (GraphPad Software Inc., La Jolla, USA), Microsoft Excel 2016 (Microsoft Inc., Redmond, USA) and custom-written routines in MatLab (R2015a, MathWorks Inc., Natwick, USA) were employed. Unless otherwise stated, data is expressed as the mean \pm S.D. Group statistics were calculated using unpaired nonparametric Kolmogorov-Smirnov test: *= $p < 0.05$, **= $p < 0.01$, ***= $p < 0.001$, ****= $p < 0.0001$, n.s.=non-significant. Correlation tables were calculated using non-parametric Spearman's r at a significance level of $p < 0.05$.

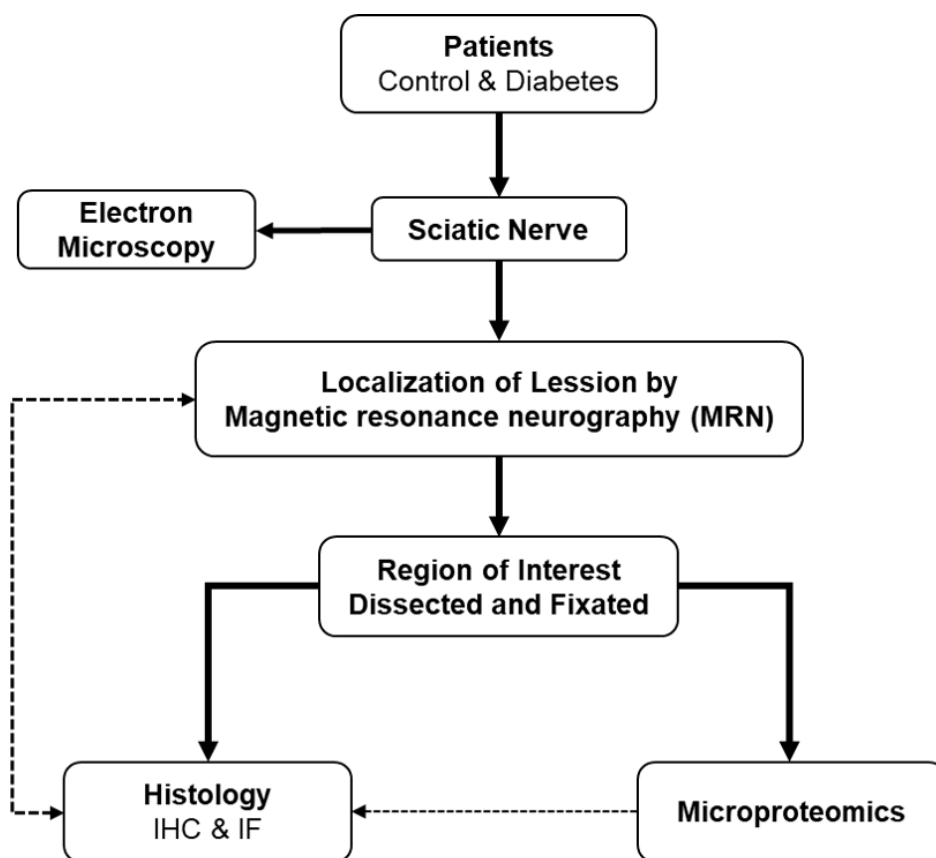
References

1. Levey AS, Stevens LA, Schmid CH, Zhang Y (Lucy), Castro AF, Feldman HI, et al. A New Equation to Estimate Glomerular Filtration Rate. *Ann Intern Med.* 2009 May 5;150(9):604.
2. Bundesärztekammer (BÄK), Kassenärztliche Bundesvereinigung (KBV), Arbeitsgemeinschaft der Wissenschaftlichen Medizinischen Fachgesellschaften (AWMF). Nationale VersorgungsLeitlinie Neuropathie bei Diabetes im Erwachsenenalter—Langfassung. 1. Auflage. Version 5. 2011.
3. Schwarz D, Hidmark AS, Sturm V, Fischer M, Milford D, Hausser I, et al. Characterization of experimental diabetic neuropathy using multicontrast magnetic resonance neurography at ultra high field strength. *Sci Rep.* 2020 May 5;10(1):7593.
4. Schindelin J, Arganda-Carreras I, Frise E, Kaynig V, Longair M, Pietzsch T, et al. Fiji: an open-source platform for biological-image analysis. *Nat Methods.* 2012 Jul 28;9(7):676–82.

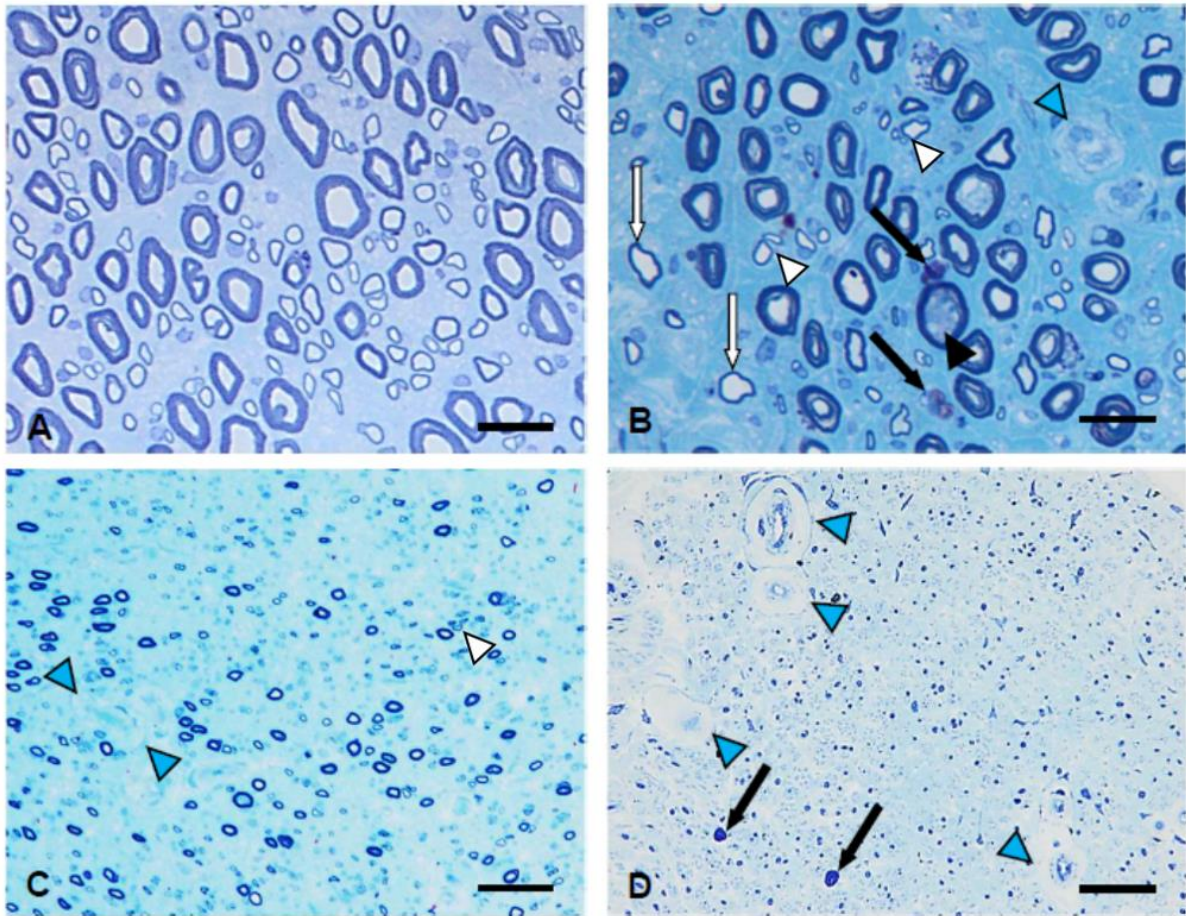
5. Pham M, Oikonomou D, Bäumer P, Bierhaus A, Heiland S, Humpert PM, et al. Proximal Neuropathic Lesions in Distal Symmetric Diabetic Polyneuropathy. *Diabetes Care*. 2011 Mar 1;34(3):721–3.
6. Morgenstern J, Groener JB, Jende JME, Kurz FT, Strom A, Göpfert J, et al. Neuron-specific biomarkers predict hypo- and hyperalgesia in individuals with diabetic peripheral neuropathy. *Diabetologia*. 2021 Dec 3;64(12):2843–55.
7. Tyanova S, Temu T, Cox J. The MaxQuant computational platform for mass spectrometry-based shotgun proteomics. *Nat Protoc*. 2016 Dec 27;11(12):2301–19.
8. Cox J, Hein MY, Luber CA, Paron I, Nagaraj N, Mann M. Accurate Proteome-wide Label-free Quantification by Delayed Normalization and Maximal Peptide Ratio Extraction, Termed MaxLFQ. *Molecular & Cellular Proteomics*. 2014 Sep;13(9):2513–26.

Supplementary Table & Figures: *In order of citation in the main text*

Supplementary Figure 1. Schematic illustrating experimental workflow in the analysis of peripheral nerve lesions in DN. IHC: Immunohistochemistry; IF: Immunofluorescence.

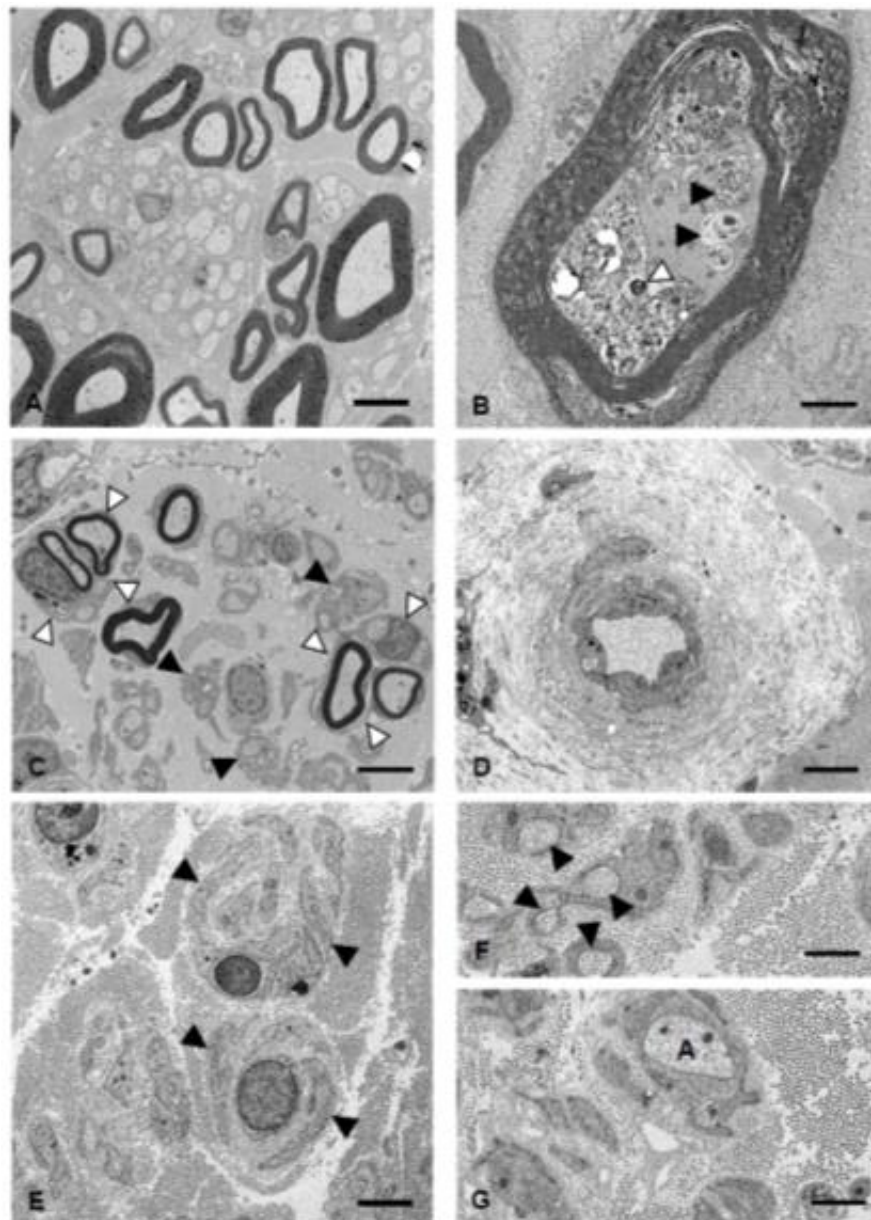


Supplementary Figure 2. Light microscopy of resin semithin sections of non-diabetic (a) and T2D (b-d) cases.



Non-diabetic case (amputation of the leg after accident). Normal density of large and small myelinated fibers. Scale bar = 5 μm (a). T2D case still minor, but progressive neuropathy, predominantly axonal. Approx. 30 % loss of large myelinated nerve fibers. Black arrowhead: axonal degeneration. Several myelin ovoids and macrophages with myelin breakdown products indicative of recent nerve fiber breakdown (black arrows). Several clusters of regenerating nerve fibers (white arrowheads) as well as axons with disproportionately thin myelin sheaths (white arrows), probably corresponding to late stage regenerating nerve fibers or secondary demyelination. Splitting of the myelin sheaths due to delayed fixation. Minor thickening of endoneurial vessel walls (blue arrowhead). Considerable endoneurial fibrosis, minor edema. Scale bar = 5 μm (b). T2D with moderately-to-severe, chronically neuropathy. Loss of 50-60% of large myelinated nerve fibers in a patchy distribution. Few groups of regenerated nerve fibers (white arrowhead). Moderate thickening of endoneurial vessel walls (blue arrowheads). Scale bar = 15 μm (c). T2D End stage neuropathy with complete loss of myelinated nerve fibers. Few myelin breakdown products (arrows). Marked thickening and hyalinization of the walls of endoneurial blood vessels (blue arrowheads). Scale bar = 15 μm (d).

Supplementary Figure 3. Electron microscopy (EM) of non-diabetic (a) and T2D (b-g) cases.

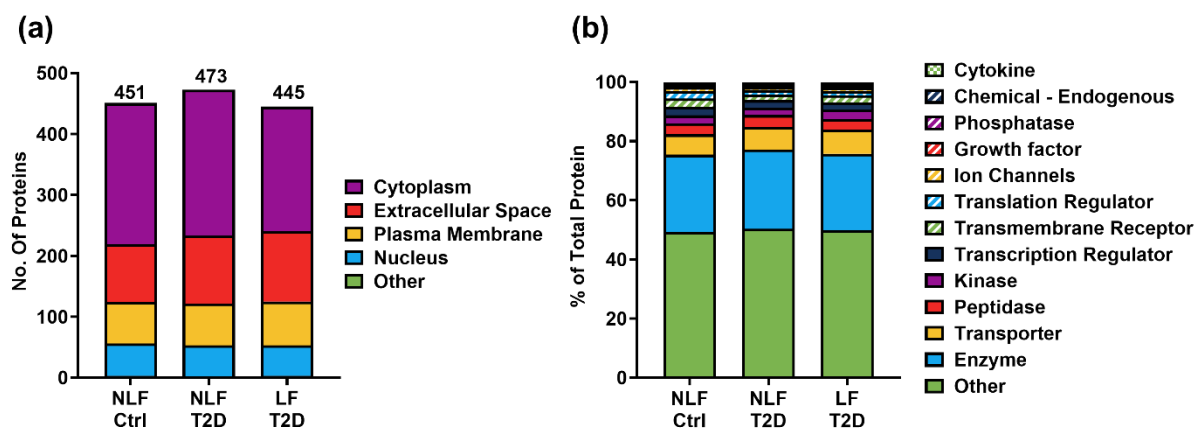


Non-diabetic case showing normal myelinated and unmyelinated nerve fibers at a normal density. Normal endoneurial collagen deposition. Scale bar = 3 μm (a). T2D with accumulation of membranous granular and membranous debris in abnormal autophagic vacuoles within an axon (black arrowheads) and in the adaxonal Schwann cell cytoplasm (white arrowhead). Scale bar = 0.8 μm (b). T2D Considerable decrease in myelinated and unmyelinated nerve fiber density. Considerable endoneurial fibrosis. Remak bundles showing reduced numbers of unmyelinated axons (black arrowheads). Two groups of regenerated nerve fibers (white arrowheads). Scale bar = 5 μm (c). Prominent thickening of the wall of an endoneurial blood vessel due to basal lamina reduplication and deposition of collagen fibers. Scale bar = 3 μm (d). Denervated Schwann cell bands (arrowheads). Marked endoneurial fibrosis. Scale bar = 2 μm (e). Collagen pockets (arrowheads) indicative of unmyelinated nerve fiber loss. Scale bar = 1 μm (f). One of the very few remaining unmyelinated axons (a) in this nerve which is otherwise almost completely devoid of nerve fibers. Scale bar = 1.2 μm (g).

Supplementary Table 1. Quantification and Correlations of Morphological and MRN Characteristics of non-lesioned fascicles (NLF) and lesioned fascicles (LF) (*Associated with Figure 1 & Figure 2*).

Parameter	NLF	LF	P-Value	Pearson correlation coefficient (r) for T2-time
Fascicle Area (μm^2)	778646 \pm 773653	3659718 \pm 1380112	<0.001	0.541 P <0.0001
Perineurium-to-fascicle ratio	0.254 \pm 0.07	0.107 \pm 0.02	<0.001	-0.542 P= 0.0001
AD-PAS Grade	1.87 \pm 0.90	3.76 \pm 0.43	<0.001	0.502 P <0.0001
T2-time (ms)	25.4 \pm 4.65	46.5 \pm 5.52	<0.001	
Fractional Anisotropy (FA)	0.342 \pm 0.06	0.197 \pm 0.06	<0.001	
Apparent Diffusion Coefficient (ADC; $\times 10^{-3} \text{ mm}^2/\text{s}$)	0.0013 \pm 0.0003	0.0018 \pm 0.0001	<0.001	
Magnetization Transfer Contrast (MTC)	0.196 \pm 0.03	0.151 \pm 0.03	<0.001	
PGP9.5 ⁺ Axons (Diameter-to-Number Ratio)	45.7 \pm 9.2	54.3 \pm 27.1	>0.999	
MBP ⁺ Axons (Diameter-to-Number Ratio)	52.2 \pm 27.4	11.8 \pm 8.02	<0.0001	
NFL ⁺ Axons (Diameter-to-Number Ratio)	24.0 \pm 9.61	16.2 \pm 6.71	<0.05	

Supplementary Figure 4. Total number of proteins quantified and their respective subcellular location in the NLF-Ctrl, NLF-T2D and LF-T2D **(a)**. The classification and relative distribution of the functions of the proteins quantified in each of the groups **(b)** (*Associated with Figure 3*).



Supplementary Information: Schwarz et al., Exploring Structural and Molecular Features of Sciatic Nerve Lesions in Diabetic Neuropathy: Unveiling Pathogenic Pathways and Targets

Supplementary Table 2. List of differentially changed proteins in NLF-T2D fascicles with respect to NLF-Ctrl (*Associated with Figure 3c*).

Protein Name	Symbol	Location	Type(s)	Log ₂ [FC]	Adjusted P-value
Upregulated					
Hemoglobin subunit alpha 2	HBA1	Extracellular Space	Transporter	2.364	3.09E-09
Complement factor B	CFB	Extracellular Space	Peptidase	1.549	3.16E-06
Serpin family A member 1	SERPINA1	Extracellular Space	Other	1.266	7.91E-04
Transferrin	TF	Extracellular Space	Transporter	1.109	2.51E-04
Downregulated					
Ferritin light chain	FTL	Cytoplasm	Enzyme	-1.164	1.42E-03
Immunoglobulin heavy constant alpha 1	IGHA1	Extracellular Space	Other	-1.979	1.81E-09

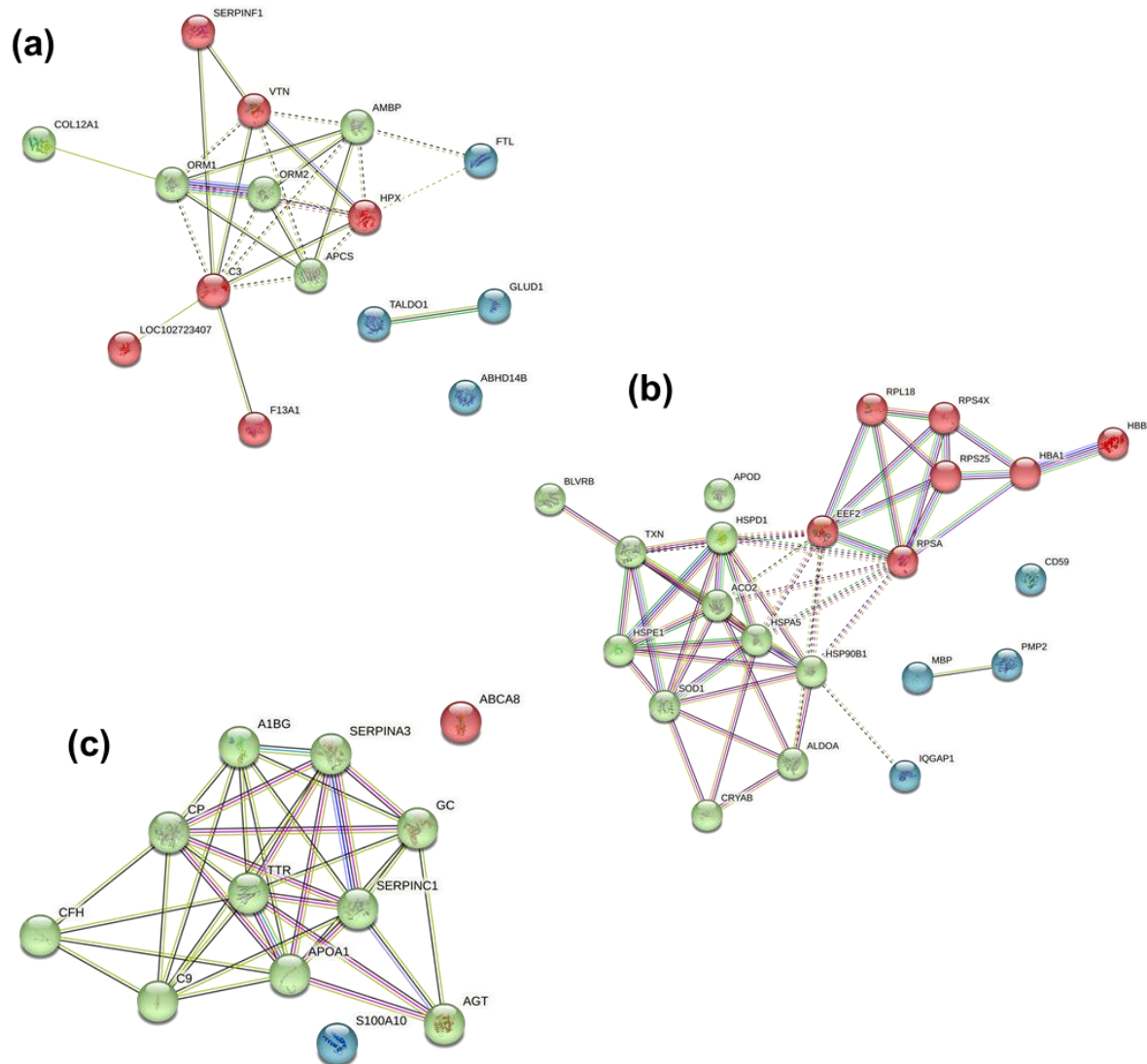
Supplementary Table 3a. List of differentially changed proteins in LF-T2D with respect to NLF-Ctrl (*Associated with Figure 3c*). Proteins highlighted in bold were also identified in the comparison with NLF-T2D.

Protein Name	Symbol	Location	Type(s)	Log ₂ [FC]	Adjusted P-value
Upregulated					
Hemopexin	HPX	Extracellular Space	Transporter	2.558	1.21E-04
Alpha-1-microglobulin/bikunin precursor	AMBP	Extracellular Space	Transporter	2.103	1.54E-11
Orosomucoid 2	ORM2	Extracellular Space	Other	1.738	1.73E-02
Vitronectin	VTN	Extracellular Space	Other	1.645	1.00E-15
Orosomucoid 1	ORM1	Extracellular Space	Other	1.615	4.86E-03
Complement C3	C3	Extracellular Space	Peptidase	1.461	1.00E-15
Abhydrolase domain containing 14B	ABHD14B	Cytoplasm	Enzyme	1.331	1.11E-07
Serpin family F member 1	SERPINF1	Extracellular Space	Other	1.245	1.96E-07
Transaldolase 1	TALDO1	Cytoplasm	Enzyme	1.151	4.04E-03
Downregulated					
Heat shock protein family D (Hsp60) member 1	HSPD1	Cytoplasm	Enzyme	-1.019	1.90E-05
Aldolase, fructose-bisphosphate A	ALDOA	Cytoplasm	Enzyme	-1.036	1.96E-04
Superoxide dismutase, type 1	SOD1	Cytoplasm	Enzyme	-1.041	1.97E-04
10 kDa heat shock protein, mitochondrial	HSPE1	Membrane	Enzyme	-1.042	3.56E-05
Apolipoprotein D	APOD	Extracellular Space	Transporter	-1.044	5.53E-04
Ras GTPase-activating-like protein IQGAP1	IQGAP1	Membrane	Other	-1.050	1.23E-12
Eukaryotic elongation factor 2	EEF2	Cytoplasm	Enzyme	-1.082	3.11E-04
CD59 molecule (CD59 blood group)	CD59	Membrane	Other	-1.085	8.82E-05
Biliverdin reductase B	BLVRB	Cytoplasm	Enzyme	-1.112	3.88E-05
Tibosomal protein S4 X-linked	RPS4X	Cytoplasm	Other	-1.135	1.66E-04
60S ribosomal protein L18	RPL18	Cytoplasm	Other	-1.142	9.10E-05
Heat shock protein 90 beta family member 1	HSP90B1	Cytoplasm	Other	-1.149	8.72E-07
Crystallin alpha B	CRYAB	Nucleus	Other	-1.158	4.68E-05
Peripheral Myelin Protein 2	PMP2	Extracellular Space	Other	-1.163	2.25E-02
40S ribosomal protein S25 (eS25)	RPS25	Cytoplasm	Other	-1.176	3.68E-03
Ribosomal protein SA	RPSA	Cytoplasm	Translation regulator	-1.231	7.34E-05
Myelin basic protein	MBP	Extracellular Space	Other	-1.257	4.09E-02
Heat shock protein family A (Hsp70) member 5	HSPA5	Cytoplasm	Enzyme	-1.398	1.83E-04
Thioredoxin	TXN	Cytoplasm	Other	-1.439	2.32E-05

Supplementary Table 3b. List of differentially changed proteins in LF-T2D with respect to NLF-T2D (*Associated with Figure 3c*). Proteins highlighted in bold were also identified in the comparison with NLF-Ctrl.

Protein Name	Symbol	Location	Type(s)	Log ₂ [FC]	Adjusted P-value
Upregulated					
Immunoglobulin heavy constant alpha 1	IGHA1	Extracellular Space	Other	2.416	1.35E-09
Alpha-1-microglobulin/bikunin precursor	AMBP	Extracellular Space	Transporter	1.754	2.83E-09
Ferritin light chain	FTL	Cytoplasm	Enzyme	1.614	1.05E-09
Amyloid P component, serum	APCS	Extracellular Space	Other	1.614	1.99E-11
Coagulation factor XIII A chain	F13A1	Extracellular Space	Enzyme	1.257	8.00E-15
Collagen type XII alpha 1 chain	COL12A1	Extracellular Space	Other	1.187	2.37E-07
Immunoglobulin heavy constant gamma 1 (G1m marker)	IGHG1	Extracellular Space	Other	1.043	3.68E-05
Glutamate dehydrogenase 2, mitochondrial	GLUD1/2	Cytoplasm	Enzyme	1.029	2.74E-08
Downregulated					
Biliverdin reductase B	BLVRB	Cytoplasm	Enzyme	-1.005	4.07E-05
Aconitase 2	ACO2	Cytoplasm	Enzyme	-1.095	2.92E-05
Hemoglobin subunit alpha 2	HBA1	Extracellular Space	Transporter	-2.750	1.00E-15
Hemoglobin subunit beta	HBB	Extracellular Space	Transporter	-2.938	5.41E-04

Supplementary Figure 5. STRING analysis of the predicted protein-protein interactions and functional clustering of the 17 upregulated proteins specific to LF-T2D (**a**; *Associated with Supplementary Table 4a & 4b*); the 23 downregulated proteins specific to the LF-T2D (**b**; *Associated with Supplementary Table 4a & 4b*); and the 12 upregulated proteins shared by NLF-T2D and LF-T2D, relative to NLF-Ctrl (**c**; *Associated with Supplementary Table 5*). Cluster one is shown in red; Cluster two is shown in green and cluster three is shown in blue.



Legend:

Red line - indicates the presence of fusion evidence
 Green line - neighborhood evidence
 Blue line - cooccurrence evidence
 Purple line - experimental evidence
 Yellow line - textmining evidence
 Light blue line - database evidence
 Black line - coexpression evidence.

Supplementary Table 4. List of differentially changes proteins shared between NLF-T2D and LF-T2D, with respect to NLF-Ctrl (*Associated with Figure 3c*).

Protein Name	Symbol	Location	Type(s)	NLF-Ctrl vs. NLF-T2D		NLF-Ctrl vs. LF-T2D	
				Log ₂ [FC]	Adjusted P-value	Log ₂ [FC]	Adjusted P-value
Upregulated							
Ceruloplasmin	CP	Extracellular Space	Enzyme	3.043	1.00E-15	3.455	1.00E-15
Apolipoprotein A1	APOA1	Extracellular Space	Transporter	1.941	4.10E-07	2.214	2.00E-15
GC vitamin D binding protein	GC	Extracellular Space	Transporter	1.548	7.74E-09	1.428	1.98E-12
Transthyretin	TTR	Extracellular Space	Transporter	1.524	1.88E-07	1.748	5.73E-13
Alpha-1-B glycoprotein	A1BG	Extracellular Space	Other	1.463	2.33E-07	1.617	4.81E-13
Serpin family C member 1	SERPINC1	Extracellular Space	Enzyme	1.258	1.06E-03	1.754	1.09E-10
Angiotensinogen	AGT	Extracellular Space	Growth Factor	1.160	7.25E-03	1.203	8.36E-03
Serpin family A member 3	SERPINA3	Extracellular Space	Other	1.158	6.08E-04	1.172	3.51E-05
ATP binding cassette subfamily A member 8	ABCA8	Plasma Membrane	Transporter	1.142	8.17E-05	1.380	3.58E-09
Complement factor H	CFH	Extracellular Space	Other	1.132	1.39E-07	1.523	1.00E-15
Complement C9	C9	Extracellular Space	Other	1.128	6.94E-05	1.716	7.05E-13
S100 calcium binding protein A10	S100A10	Cytoplasm	Other	1.119	3.45E-06	1.495	6.30E-14
Downregulated							
Cathepsin D	CTSD	Other	Peptidase	-1.263	9.85E-03	-1.660	6.64E-08
Fatty Acid Binding Protein 5	FABP5	Cytoplasm	Transporter	-1.453	8.33E-03	-1.975	2.93E-08

Supplementary Table 5. Log2 transformed label-free quantification (LFQ) intensities for complement proteins and immunoglobulin subtypes in NLF-Ctrl (N = 5), NLF-T2D (N = 6) and LF-T2D (N=55). Data represents mean \pm SD; ****P < 0.0001, **P < 0.01, *P < 0.05 versus NLF-Ctrl; +++P < 0.0001; ++P < 0.01 versus NLF-T2D.

	Log2(LFQ Intensity)		
	NLF-Ctrl	NLF-T2D	LF-T2D
Complement Proteins			
C3	28.5 \pm 2.2	30.3 \pm 0.4****	30.8 \pm 0.5****
C9	24.8 \pm 1.2	26.3 \pm 0.4****	26.8 \pm 0.5****
CD59	27.2 \pm 0.3	27.1 \pm 0.4	26.1 \pm 0.4****/+++
Immunoglobulin Subtypes			
IgG1	30.7 \pm 1.2	30.8 \pm 0.3	31.9 \pm 0.4****/+++
IgG2	28.4 \pm 1.6	28.5 \pm 1.1	29.5 \pm 0.7**/++
IgG3	28.7 \pm 1.6	28.6 \pm 1.9	29.1 \pm 0.7
IgA1	29.5 \pm 1.6	28.0 \pm 0.5*	30.1 \pm 1.1++++

Supplementary Information: Schwarz et al., Exploring Structural and Molecular Features of Sciatic Nerve Lesions in Diabetic Neuropathy: Unveiling Pathogenic Pathways and Targets

Supplementary Table 6a. List of the 32 unique proteins identified in the NLF-Ctrl (*Associated with Figure 3 & Supplementary Figure 5a*).

Name	Symbol	Location	Type(s)
ADP ribosylation factor like GTPase 6 interacting protein 5	ARL6IP5	Cytoplasm	Other
Calreticulin	CALR	Cytoplasm	Transcription regulator
Capping actin protein of muscle Z-line subunit alpha 1	CAPZA1	Cytoplasm	Other
CD14 molecule	CD14	Plasma Membrane	Transmembrane receptor
Chloride intracellular channel 1	CLIC1	Nucleus	Ion channel
Cathepsin B	CTSB	Cytoplasm	Peptidase
Cytochrome b5 type A	CYB5A	Cytoplasm	Enzyme
Dystrophin related protein 2	DRP2	Plasma Membrane	Other
Desmocollin 1	DSC1	Plasma Membrane	Other
Desmoplakin	DSP	Plasma Membrane	Other
Eukaryotic translation elongation factor 1 delta	EEF1D	Cytoplasm	Transcription regulator
Eukaryotic translation initiation factor 3 subunit A	EIF3A	Cytoplasm	Transcription regulator
G protein subunit alpha 13	GNA13	Plasma Membrane	Enzyme
Glypican 1	GPC1	Plasma Membrane	Transmembrane receptor
Glutathione peroxidase 3	GPX3	Extracellular Space	Enzyme
Hypoxia up-regulated 1	HYOU1	Cytoplasm	Other
Integrin subunit alpha V	ITGAV	Plasma Membrane	Transmembrane receptor
Lysosomal associated membrane protein 1	LAMP1	Plasma Membrane	Other
Niban apoptosis regulator 2	NIBAN2	Cytoplasm	Transcription regulator
N-ethylmaleimide sensitive factor, vesicle fusing ATPase	NSF	Cytoplasm	Transporter
Poly(A) binding protein Cic 1	PABPC1	Cytoplasm	Transcription regulator
Progesterone receptor membrane component 2	PGRMC2	Nucleus	Transporter
Arginyl aminopeptidase	RNPEP	Cytoplasm	Peptidase
Ribosomal protein L10a	RPL10A	Nucleus	Other
Ribosomal protein L23a	RPL23A	Cytoplasm	Other
Ribosomal protein S9	RPS9	Cytoplasm	Translation regulator
S100 calcium binding protein A1	S100A1	Cytoplasm	Other
Saccharopine dehydrogenase (putative)	SCCPDH	Cytoplasm	Other
Selenium binding protein 1	SELENBP1	Cytoplasm	Other
Stathmin 2	STMN2	Plasma Membrane	Other
Transglutaminase 3	TGM3	Cytoplasm	Enzyme
Thymosin beta 4 X-linked	TMSB10/TMSB4X	Cytoplasm	Other
Tubulin beta 6 class V	TUBB6	Cytoplasm	Other

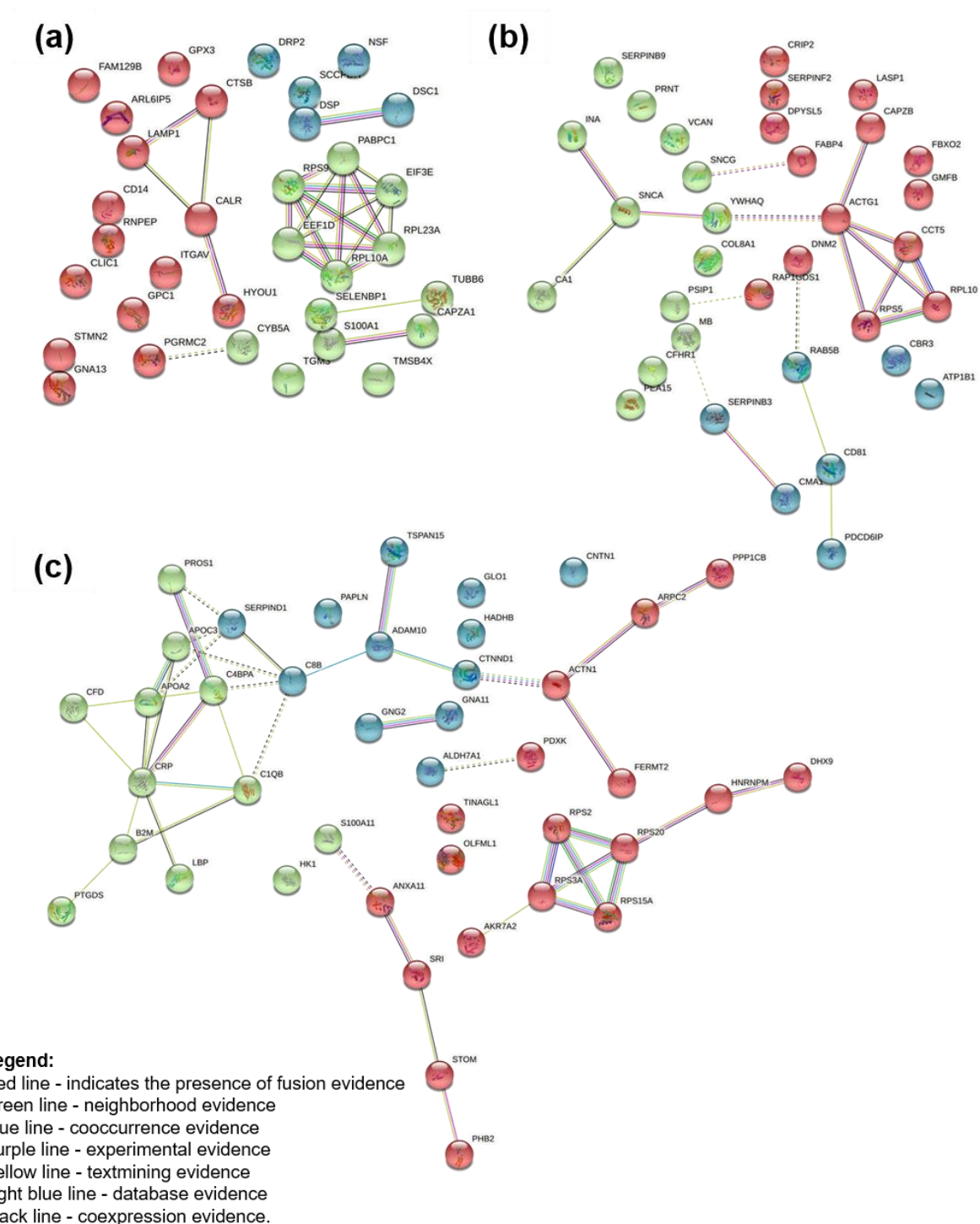
Supplementary Table 6b. List of the 37 unique proteins identified in the NLF-T2D (*Associated with Figure 3 & Supplementary Figure 5b*).

Name	Symbol	Location	Type(s)
Actin gamma 1	ACTG1	Cytoplasm	Other
ATPase Na ⁺ /K ⁺ transporting subunit beta 1	ATP1B1	Plasma Membrane	Transporter
Carbonic anhydrase 1	CA1	Cytoplasm	Enzyme
Capping actin protein of muscle Z-line subunit beta	CAPZB	Cytoplasm	Other
Carbonyl reductase 3	CBR3	Cytoplasm	Enzyme
Chaperonin containing TCP1 subunit 5	CCT5	Cytoplasm	Other
CD81 molecule	CD81	Plasma Membrane	Other
complement factor H related 1	CFHR1	Extracellular Space	Other
Chymase 1	CMA1	Extracellular Space	Peptidase
Collagen type VIII alpha 1 chain	COL8A1	Extracellular Space	Other
Cysteine rich protein 2	CRIP2	Nucleus	Other
Dynamin 2	DNM2	Plasma Membrane	Enzyme
Dihydropyrimidinase like 5	DPYSL5	Cytoplasm	Enzyme
Fatty acid binding protein 4	FABP4	Cytoplasm	Transporter
F-box protein 2	FBXO2	Cytoplasm	Enzyme
Glia maturation factor beta	GMFB	Cytoplasm	Growth factor
Internexin neuronal intermediate filament protein alpha	INA	Cytoplasm	Other
LIM and SH3 protein 1	LASP1	Cytoplasm	Transporter
Myoglobin	MB	Cytoplasm	Transporter
Programmed cell death 6 interacting protein	PDCD6IP	Cytoplasm	Other
Proliferation and apoptosis adaptor protein 15	PEA15	Cytoplasm	Transporter
Prion protein	PRNP	Plasma Membrane	Other
PC4 and SFRS1 interacting protein 1	PSIP1	Nucleus	Transcription regulator
RAB5B, member RAS oncogene family	RAB5B	Cytoplasm	Enzyme
Rap1 GTPase-GDP dissociation stimulator 1	RAP1GDS1	Cytoplasm	Other
Ribosomal protein L10	RPL10	Cytoplasm	Transcription regulator
Ribosomal protein S5	RPS5	Cytoplasm	Other
Serpin family B member 3	SERPINB3	Cytoplasm	Other
Serpin family B member 9	SERPINB9	Cytoplasm	Other
Serpin family F member 2	SERPINF2	Extracellular Space	Other
Synuclein alpha	SNCA	Cytoplasm	Enzyme
Synuclein gamma	SNCG	Cytoplasm	Other
Versican	VCAN	Extracellular Space	Other
Tyrosine 3-monooxygenase/tryptophan 5-monooxygenase activation protein theta	YWHAQ	Cytoplasm	Other

Supplementary Table 6c. List of the 43 unique proteins identified in the LF-T2D (*Associated with Figure 3 & Supplementary Figure 5c*).

Name	Symbol	Location	Type(s)
Actinin alpha 1	ACTN1	Cytoplasm	Transcription regulator
ADAM metallopeptidase domain 10	ADAM10	Plasma Membrane	Peptidase
Aldo-keto reductase family 7 member A2	AKR7A2	Cytoplasm	Enzyme
Aldehyde dehydrogenase 7 family member A1	ALDH7A1	Cytoplasm	Enzyme
Annexin A11	ANXA11	Nucleus	Other
Apolipoprotein A2	APOA2	Extracellular Space	Transporter
Apolipoprotein C3	APOC3	Extracellular Space	Transporter
Actin related protein 2/3 complex subunit 2	ARPC2	Cytoplasm	Other
Beta-2-microglobulin	B2M	Plasma Membrane	transmembrane receptor
Complement C1q B chain	C1QB	Extracellular Space	Other
Complement component 4 binding protein alpha	C4BPA	Extracellular Space	Other
Complement C8 beta chain	C8B	Extracellular Space	Other
Complement factor D	CFD	Extracellular Space	Peptidase
Contactin 1	CNTN1	Plasma Membrane	Enzyme
C-reactive protein	CRP	Extracellular Space	Other
Catenin delta 1	CTNND1	Nucleus	Other
DEXH-box helicase 9	DHX9	Nucleus	Enzyme
FERM domain containing kindlin 2	FERMT2	Cytoplasm	Other
Glyoxalase I	GLO1	Cytoplasm	Enzyme
G protein subunit alpha 11	GNA11	Plasma Membrane	Enzyme
G protein subunit gamma 2	GNG2	Plasma Membrane	Enzyme
Ribosomal protein S15a	RPS15A	Cytoplasm	Other
Hexokinase 1	HK1	Cytoplasm	kinase
Heterogeneous nuclear ribonucleoprotein M	HNRNPM	Nucleus	Other
Lipopolysaccharide binding protein	LBP	Plasma Membrane	Transporter
Olfactomedin like 1	OLFML1	Extracellular Space	Other
Papilin, proteoglycan like sulfated glycoprotein	PAPLN	Extracellular Space	Other
Pyridoxal kinase	PDXK	Cytoplasm	kinase
Prohibitin 2	PHB2	Cytoplasm	Transcription regulator
Protein phosphatase 1 catalytic subunit beta	PPP1CB	Cytoplasm	Phosphatase
Protein S	PROS1	Extracellular Space	Other
Prostaglandin D2 synthase	PTGDS	Cytoplasm	Enzyme
Ribosomal protein S2	RPS2	Cytoplasm	Other
Hydroxyacyl-CoA dehydrogenase trifunctional multienzyme complex subunit beta	HADHB	Cytoplasm	Enzyme
Ribosomal protein S20	RPS20	Cytoplasm	Other
Ribosomal protein S3A	RPS3A	Nucleus	Other
S100 calcium binding protein A11	S100A11	Cytoplasm	Other
Serpin family D member 1	SERPIND1	Extracellular Space	Other
Sorcin	SRI	Cytoplasm	Transporter
Stomatin	STOM	Plasma Membrane	Other
Tubulointerstitial nephritis antigen like 1	TINAGL1	Extracellular Space	Transporter
Tetraspanin 15	TSPAN15	Plasma Membrane	Other

Supplementary Figure 6. STRING analysis of the predicted protein-protein interactions and functional clustering of the 32 unique proteins identified in NLF-Ctrl (a) (*Associated with Supplementary Tables 6a & 7a*); the 37 unique proteins identified in the NLF-T2D (b) (*Associated with Supplementary Tables 6b & 7b*), and the 43 unique proteins identified in the LF-T2D (c) (*Associated with Supplementary Tables 6c & 7c*). Cluster one is shown in red; Cluster two is shown in green and cluster three is shown in blue.



Supplementary Information: Schwarz et al., Exploring Structural and Molecular Features of Sciatic Nerve Lesions in Diabetic Neuropathy: Unveiling Pathogenic Pathways and Targets

Supplementary Table 7a. Functional and biological functional pathways identified for the 32 unique proteins identified in the NLF-Ctrl (*Associated with Supplementary Table 6a & Supplementary Figure 5a*).

GO Term	Term Description	Observed Protein Count	Background Protein Count	Strength	False Discovery Rate (FDR)
Cluster 1					
GO:0031982	Vesicle	8	3957	0.70	0.0023
GO:0070062	Extracellular exosome	7	2096	0.92	0.0023
GO:0044194	Cytolytic granule	2	12	2.61	0.0045
GO:0071682	Endocytic vesicle lumen	2	23	2.33	0.0110
GO:0005790	Smooth endoplasmic reticulum	2	30	2.22	0.0162
GO:0048471	Perinuclear region of cytoplasm	4	727	1.13	0.0239
GO:0030139	Endocytic vesicle	3	338	1.34	0.0460
Cluster 2					
GO:0045182	Translation regulator activity	4	152	1.94	0.00028
GO:0090079	Translation regulator activity, nucleic acid binding	3	121	1.91	0.0118
GO:0003735	Structural constituent of ribosome	3	169	1.77	0.0211
GO:0003723	RNA binding	5	1672	0.99	0.0305
GO:0005198	Structural molecule activity	4	776	1.23	0.0338
Cluster 3					
GO:0031982	Vesicle	8	3957	0.70	0.0023
GO:0070062	Extracellular exosome	7	2096	0.92	0.0023
GO:0044194	Cytolytic granule	2	12	2.61	0.0045
GO:0071682	Endocytic vesicle lumen	2	23	2.33	0.0110
GO:0005790	Smooth endoplasmic reticulum	2	30	2.22	0.0162
GO:0048471	Perinuclear region of cytoplasm	4	727	1.13	0.0239
GO:0030139	Endocytic vesicle	3	338	1.34	0.0460

Supplementary Information: Schwarz et al., Exploring Structural and Molecular Features of Sciatic Nerve Lesions in Diabetic Neuropathy: Unveiling Pathogenic Pathways and Targets

Supplementary Table 7b. Functional and biological functional pathways identified for the 37 unique proteins identified in the NLF-T2D (*Associated with Supplementary Table 6b & Supplementary Figure 5b*).

GO Term	Term Description	Observed Protein Count	Background Protein Count	Strength	False Discovery Rate (FDR)
Cluster 1					
GO:0005576	Extracellular region	11	4166	0.60	0.0035
GO:0005615	Extracellular space	10	3195	0.67	0.0035
Cluster 2					
GO:0005576	Extracellular region	11	4166	0.6	0.0035
GO:0005615	Extracellular space	10	3195	0.67	0.0035
Cluster 3					
GO:0005615	Extracellular space	7	3195	0.79	0.0053
GO:0001772	Immunological synapse	2	37	2.18	0.0457

Supplementary Table 7c. Functional and biological functional pathways identified for the 43 unique proteins identified in the LF-T2D (*Associated with Supplementary Table 6c & Supplementary Figure 5c*).

GO Term	Term Description	Observed Protein Count	Background Protein Count	Strength	False Discovery Rate (FDR)
Cluster 1					
GO:0000380	Alternative mRNA splicing, via spliceosome	2	18	2.19	0.046
GO:0019083	Viral transcription	5	115	1.78	0.0002
GO:0006614	SRP-dependent cotranslational protein targeting to membrane	4	96	1.77	0.0026
GO:0000184	Nuclear-transcribed mRNA catabolic process, nonsense-mediated decay	4	119	1.67	0.0026
GO:0006413	Translational initiation	4	141	1.6	0.0038
GO:0072594	Establishment of protein localization to organelle	5	433	1.21	0.0078
GO:0006518	Peptide metabolic process	5	503	1.14	0.0116
Cluster 2					
GO:0097197	Tetraspanin-enriched microdomain	2	10	2.45	0.0059
GO:0005834	Heterotrimeric G-protein complex	2	33	1.93	0.0265
GO:0031234	Extrinsic component of cytoplasmic side of plasma membrane	3	94	1.65	0.007
GO:0019897	Extrinsic component of plasma membrane	4	166	1.53	0.0039
GO:0030027	Lamellipodium	3	202	1.32	0.0306
GO:0005925	Focal adhesion	5	405	1.24	0.0039
GO:0098978	Glutamatergic synapse	4	361	1.19	0.0124
GO:0031252	Cell leading edge	4	425	1.12	0.0207
Cluster 3					
GO:0060621	Negative regulation of cholesterol import	2	2	3.18	0.001
GO:0010903	Negative regulation of very-low-density lipoprotein particle remodeling	2	3	3.00	0.002
GO:0008228	Opsonization	2	9	2.52	0.007
GO:0034371	Chylomicron remodeling	2	9	2.52	0.007
GO:0034378	Chylomicron assembly	2	10	2.48	0.008
GO:0033700	Phospholipid efflux	2	12	2.40	0.011
GO:0006957	Complement activation, alternative pathway	2	13	2.36	0.012
GO:0043691	Reverse cholesterol transport	2	17	2.25	0.017
GO:0060192	Negative regulation of lipase activity	2	17	2.25	0.017
GO:0034375	High-density lipoprotein particle remodeling	2	18	2.22	0.018
GO:0006958	Complement activation, classical pathway	4	38	2.20	0.000
GO:0006956	Complement activation	5	54	2.14	0.000
GO:0033344	Cholesterol efflux	2	23	2.12	0.028
GO:0050995	Negative regulation of lipid catabolic process	2	24	2.10	0.029
GO:0030449	Regulation of complement activation	4	56	2.03	0.000